Cone-Beam Reconstruction of Objects with Localized Heterogeneities

Frank Dennerlein, Frédéric Noo

I. Introduction

Circular cone-beam (CB) computed tomography has become an attractive imaging method, not only for medical applications but also for non-destructive testing. A popular algorithm for reconstruction from CB data of a full circular scan has been suggested by Feldkamp *et al.* (FDK) [1]. FDK yields acceptable image quality in various practical scenarios. However, when using FDK for imaging objects that contain strong density variations in z, a significant level of CB artifacts can be observed. Typically, these artifacts spread over wide regions of the reconstructed volume, even when the strong variations in z are very localized within the object.

In this paper, we introduce and evaluate a novel analytical reconstruction formula that produces in some scenarios results of a quality superior to that of FDK. In particular, a significant artifact reduction is achieved for objects which contain structures that have high-magnitude along z, but are localized in x and y

II. Notation and Reconstruction Theory

Our objective is to recover the density function $f(\underline{x})$ with $\underline{x} = (x, y, z)$ of an object that is interrogated by a CT scanning device. During the scan, the X-ray source moves along the circular trajectory $\underline{a}(\lambda) = (R\cos\lambda, R\sin\lambda, 0)$, where R denotes the radius of the circle and $\lambda \in [0, 2\pi)$ describes the polar angle of the source. We assume a planar X-ray detector that is described using the orthonormal system $\underline{e}_u(\lambda) = (-\sin\lambda, \cos\lambda, 0)$, $\underline{e}_v(\lambda) = (0, 0, 1)$ and $\underline{e}_w(\lambda) = (\cos\lambda, \sin\lambda, 0)$. The detector plane is spanned by $\underline{e}_u(\lambda)$ and $\underline{e}_v(\lambda)$ and is at distance D from the source. A location on the detector is specified using coordinates u and $v \in [-v_m, v_m]$ that are measured along these two axis, respectively. CB data acquisition yields the function $g(\lambda, u, v)$ that describes integrals of f along rays that start at $\underline{a}(\lambda)$ and intersects the detector at coordinates (u, v). We now suggest to reconstruct

$$\hat{f}(\underline{x}) = -\frac{1}{8\pi}\int_0^{2\pi} d\lambda \, \frac{1}{R - \underline{x}\cdot\underline{e}_w(\lambda)} g_F(\lambda, u^*, v^*). \tag{1}$$

as an approximation of $f(\underline{x})$. In this expression, u^* and v^* define the detector coordinates of the CB projection of $\underline{x}$ at source position λ and

$$\begin{aligned} g_F(\lambda, u^*, v^*) = \int_{-\infty}^{\infty} du \, \frac{1}{\pi(u^* - u)} \times \\ \big(\tilde{g}^e(\lambda, u, v^* + m_1^*(u - u^*)) + \tilde{g}^e(\lambda, u, v^* + m_2^*(u - u^*))\big). \end{aligned} \tag{2}$$

denotes filtered CB data. Furthermore,

$$\tilde{g}^e(\lambda, u, v) = \begin{cases} D\tilde{g}(\lambda, u, -v_m)/\sqrt{u^2 + v_m^2 + D^2} & \text{if } v < -v_m \\ D\tilde{g}(\lambda, u, v_m)/\sqrt{u^2 + v_m^2 + D^2} & \text{if } v > v_m \\ D\tilde{g}(\lambda, u, v)/\sqrt{u^2 + v^2 + D^2} & \text{otherwise.} \end{cases} \tag{3}$$

while $\tilde{g}(\cdot, \cdot, \cdot)$ describes CB data differentiated in λ at fixed ray direction. The filtering equation (2) defines a Hilbert transform along two lines through (u^*, v^*) with slopes

$$m_1^* = \frac{(\underline{x} - \underline{a}(\lambda_A))\cdot\underline{e}_v(\lambda)}{(\underline{x} - \underline{a}(\lambda_A))\cdot\underline{e}_u(\lambda)} \qquad m_2^* = \frac{(\underline{x} - \underline{a}(\lambda_B))\cdot\underline{e}_v(\lambda)}{(\underline{x} - \underline{a}(\lambda_B))\cdot\underline{e}_u(\lambda)} \tag{4}$$

The parameters $\lambda_A \in [0, 2\pi)$ and $\lambda_B \in [0, 2\pi)$ are here selected individually for each point $\underline{x}$, such that $\underline{x}$, $\underline{a}(\lambda_A)$ and $\underline{a}(\lambda_B)$ define a plane orthogonal to the PCS and such that the parameters λ_A and $\lambda_B > \lambda_A$ minimize the expression

$$\begin{aligned} c(\lambda_1, \lambda_2) = \left[\int_{-v_m}^{v_m} dv \, \left(\frac{\partial}{\partial v}\frac{D\, g(\lambda_1, u^*, v)}{\sqrt{u^{*2} + v^2 + D^2}}\right)^2\right]^{\frac{1}{2}} \\ + \left[\int_{-v_m}^{v_m} dv \, \left(\frac{\partial}{\partial v}\frac{D\, g(\lambda_2, u^*, v)}{\sqrt{u^{*2} + v^2 + D^2}}\right)^2\right]^{\frac{1}{2}} \end{aligned} \tag{5}$$

III. Results

We simulated CB data of a tube phantom (see Fig.1) using the geometry parameters of a typical CT scanner. Our algorithm is evaluated on the task to reconstruct the region located inside the wall of the central cylinder, which has a background of 0HU and may contain varying structures. The difficulty is given by several stacks of high-attenuating discs. These surround the central cylinder and correspond to a strong density variations in z, which are, however, localized in x and y. Reconstruction results are presented in Fig. 2.

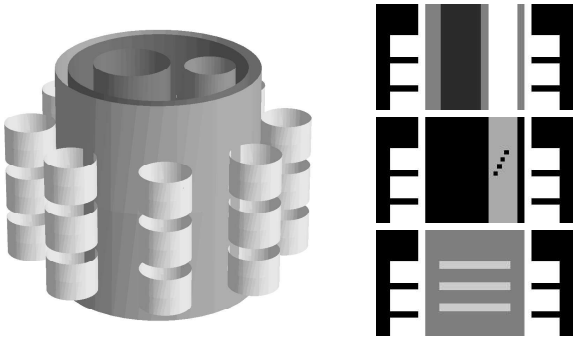

Fig. 1. (Left) 3D illustration of the tube phantom. (Right) Slice $y = 0$ through the (top) original tube phantom (grayscale window [-300HU,300HU]), (center) high-contrast tube phantom in [-50HU,550HU], (bottom) low-contrast tube phantom in [-100HU,100HU]

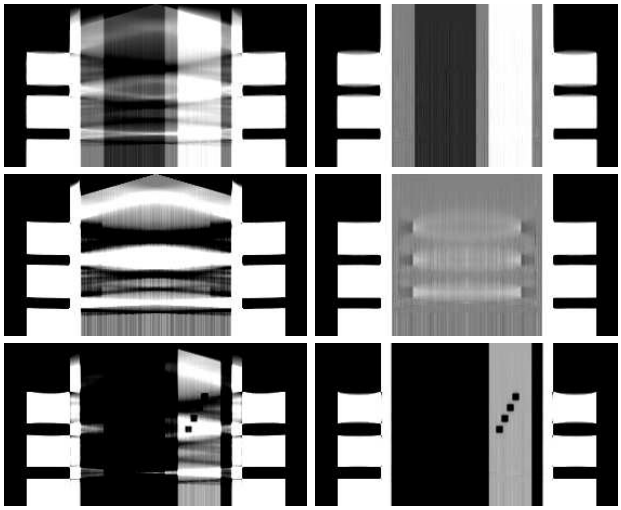

Fig. 2. Reconstructions using (left) full-scan FDK and (right) our algorithm. (Top to bottom) original tube phantom (grayscale [-300HU,+300HU]), low-contrast tube phantom ([-100HU,+100HU]) and high-contrast tube phantom ([-50HU,+550HU]).

IV. Discussion and Conclusions

The left column of Fig. 2 shows that when using the FDK method, the CB artifacts that caused by the stacks of discs spread over large areas of the object, so that an interpretation of the interior structure of the tube phantom is very difficult. Using our method, however, the CB artifacts are constricted within the regions of the discs, so that now, e.g., the inlays of the low-contrast tube phantom can be distinguished easily. In the considered scenario of imaging objects that contain high-contrast longitudinal structures which are at the smae time localized in x and y, our algorithm clearly outperforms FDK in terms of CB artifacts.

References

[1] L. A. Feldkamp, L. C. Davis, and J. W. Kress, "Practical cone beam algorithm," *Optical Society of America*, vol. 1, pp. 612–619, 1984.